Monatshefte für Chemie 138, 523–528 (2007)
DOI 10.1007/s00706-007-0663-9
Printed in The Netherlands

Monatshefte für Chemie
Chemical Monthly

The Rare Earth Metal-Rich Indides RE_4RhIn (RE=Gd–Tm, Lu)

Roman Zaremba, Ute Ch. Rodewald, Rolf-Dieter Hoffmann, and **Rainer Pöttgen***

Institut für Anorganische und Analytische Chemie, Westfälische Wilhelms-Universität Münster, Münster, Germany

Received January 2, 2007; accepted (revised) February 11, 2007; published online May 10, 2007

Summary. The rare earth-transition metal-indides RE_4RhIn (RE = Gd–Tm, Lu) were prepared by arc-melting of the elements and subsequent annealing. Single crystals were grown *via* slowly cooling of the samples. The indides were investigated *via* X-ray powder diffraction and several structures were refined from X-ray single crystal diffractometer data: $F\bar{4}3m$, $a = 1370.7(9)$ pm, $wR2 = 0.049$, 428 F^2 values for Gd_4RhIn, $a = 1360.3(6)$ pm, $wR2 = 0.028$, 420 F^2 values for Tb_4RhIn, $a = 1354.5(2)$ pm, $wR2 = 0.041$, 380 F^2 values for Dy_4RhIn, $a = 1349.2(3)$ pm, $wR2 = 0.029$, 410 F^2 values for Ho_4RhIn, $a = 1342.5(5)$ pm, $wR2 = 0.037$, 403 F^2 values for Er_4RhIn, $a = 1337.8(3)$ pm, $wR2 = 0.038$, 394 F^2 values for Tm_4RhIn with 14 variable parameters per refinement, and $a = 1329.7(3)$ pm for Lu_4RhIn. In this new structure type, the rhodium atoms have a trigonal prismatic rare earth coordination. Condensation of the RhRE_6 prisms leads to a three-dimensional network which leaves voids that are filled by regular In_4 tetrahedra (317 pm In–In distance) in Gd_4RhIn. The indium atoms have twelve nearest neighbors (3 In + 9 RE) in icosahedral coordination. The gadolinium atoms build up a three-dimensional, adamantane-like network of condensed, face-sharing empty octahedra.

Keywords. Rare earth compounds; Indides; Crystal chemistry.

Introduction

The crystal chemistry of $RE_xT_y\text{In}_z$ indides (RE = rare earth element, T = transition metal) displays three main structural characteristics: (i) If the coefficients x, y, and z are of almost equal values, the transition metal and indium atoms build up two- or three-dimensional $[T_y\text{In}_z]$ polyanionic networks which leave cages or channels for the rare earth metal atoms. Within these polyanionic networks one observes strong covalent T–In and in some cases also T–T bonding. With increasing indium content in such $[T_y\text{In}_z]$ networks, the indium atoms show segregation and the resulting indium substructures resemble the structure of elemental tetragonal body-centered indium. (ii) In the transition metal-rich part of the RE–T–In phase diagrams, compounds with one-, two- or three-dimensional transition metal substructures occur. These transition metal clusters show T–T distances close to those in the respective elements. (iii) The rare earth metal-rich structures are relatively complex and show high coordination numbers. The crystal chemistry of the $RE_xT_y\text{In}_z$ indides has recently been reviewed [1].

Among these three families of indides, those with a high rare earth metal content have only scarcely been investigated. So far, five different structure types have been observed [1]: Ho_6Co_2Ga [2], $Lu_{14}Co_2In_3$ [3–5], $Sm_{12}Ni_6In$ [6], $Ce_{12}Pt_7In$ [7], and Mo_5B_2Si [8, 9]. The common structural motif of these structure types is the trigonal prismatic coordination of the electronegative transition metal atoms by rare earth atoms. In many cases, these trigonal prisms are capped on the rectangular sites (coordination number 9), a structural motif often observed in intermetallics.

We have now started a systematic study of the rare earth metal rich parts of the RE–T–In systems, especially with the 4*d* and 5*d* transition metals with respect to crystal chemistry and magnetic properties. Herein we report on the new structure type Gd_4RhIn and the isotypic compounds RE_4RhIn (RE = Tb–Tm, Lu).

* Corresponding author. E-mail: pottgen@uni-muenster.de

Results and Discussion

New rare earth metal rich indides RE_4RhIn (RE = Gd–Tm, Lu) have been prepared and characterized by X-ray diffraction. They crystallize with a new face-centered cubic structure type, space group $F\bar{4}3m$. The lattice parameters decrease from the gadolinium to the lutetium compound (Fig. 1) as expected from the lanthanoid contraction. As an example we discuss the Gd_4RhIn structure. The latter contains three crystallographically independent gadolinium, one rhodium, and one indium site. Since this structure type has first been observed for the gadolinium compound, we consequently call it the Gd_4RhIn type.

The coordination polyhedra for Gd_4RhIn are shown in Fig. 2. The three gadolinium sites have coordination numbers (CN) 14, 14, and 15 for Gd1, Gd2, and Gd3, respectively. All gadolinium atoms have Gd, Rh, and In atoms in their coordination shell. The highest site symmetry occurs for the Gd3 site (.3m). The rhodium atoms are located in trigonal prisms formed by the Gd2 and Gd3 atoms. The most symmetrical coordination occurs for the indium atoms. They have twelve nearest neighbors in icosahedral coordination with gadolinium and indium atoms in their coordination shell.

The shortest interatomic distances in the Gd_4RhIn structure occur for Gd–Rh (284 pm), close to the sum of the covalent radii of 286 pm [19]. These can be considered as the strongest bonding interactions, in agreement wit a recent band structure calculation on isotypic La_4CoMg [15]. These trigonal $RhGd_6$ prisms are condensed *via* the edges of the triangular faces forming a rigid three-dimensional network (Fig. 3). The voids left by this network are filled by the Gd1 atoms and regular In_4 tetrahedra at In–In distances of 317 pm. The latter are even shorter than the shortest In–In distance of 325 pm in tetragonal body-centered indium [20]. Due to the high rare earth metal content we observe a clear segregation of rhodium and indium and consequently no Rh–In contacts are observed.

Together, the Gd2 and Gd3 atoms, forming the trigonal prisms, and the Gd1 atoms build up a three-dimensional network of empty, face-sharing Gd_6 octahedra (Fig. 3). Within this octahedral network,

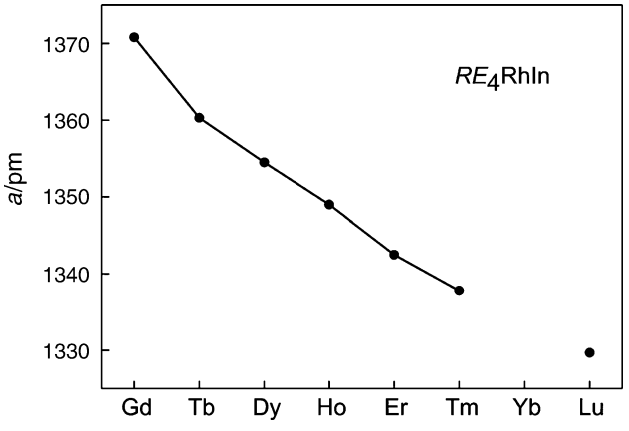

Fig. 1. Plot of the a lattice parameters of RE_4RhIn

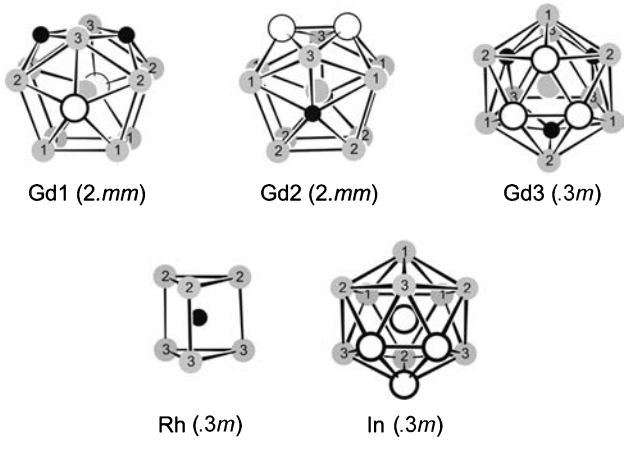

Fig. 2. Coordination polyhedra in the Gd_4RhIn structure. Atom designations and site symmetries are indicated. Gadolinium, rhodium, and indium atoms are drawn as gray, filled, and open circles

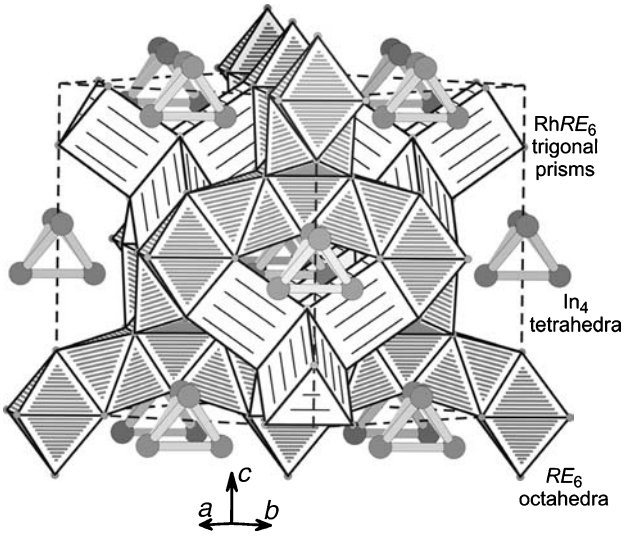

Fig. 3. View of the Gd_4RhIn structure approximately along the [110] direction. The three-dimensional networks of rhodium-centered trigonal prisms, the empty Gd_6 octahedra, and the In_4 tetrahedra are emphasized

each gadolinium atom has at least six gadolinium neighbors at Gd–Gd distances ranging from 350 to 365 pm. Several of the Gd–Gd distances are shorter than the average Gd–Gd distance of 360 pm in *hcp* gadolinium [20]. We can thus assume Gd–Gd bonding within this network. In typical cluster compounds like Gd_2Cl_3 [21–23], the Gd–Gd distances of 337 pm along the joined edges of the trans-edge sharing Gd_6 octahedra are much smaller.

Some of the centers of the Gd_6 octahedra in Gd_4RhIn are at special positions (*e.g.* 0,0,0). Some crystals investigated during the present investigation (the single crystal data are not presented here) revealed higher residual peaks (6–8 e/Å^3) at these positions and also at the site 1/4, 3/4, 3/4, where always four of the trigonal $RhGd_6$ prisms are condensed, leaving a Gd_4 tetrahedron. It is possible, that some of these voids in such crystals might be partially filled with a light element atoms, *e.g.* nitrogen or oxygen. Nevertheless, it is well known, that such highly symmetrical sites accumulate artifacts within a structure refinement (incomplete absorption correction *etc.*) and such peaks should not be overinterpreted. The compounds presented here have been obtained in amounts of 1 g in X-ray pure form, and there was no hint for any impurity content. Crystals that were grown from samples with a slightly higher rare earth content (see the Gd:Rh:In = 4.1:1:1 sample discussed above) did not reveal higher residual peaks. This might be a hint that the excess gadolinium might have trapped the light element impurities, if present at all. This behavior was not observed for the magnesium and cadmium based compounds [15, 16, 24, 25].

Keeping these empty octahedra in mind, we have recently started a systematic investigation concerning the hydrogenation behavior of the Gd_4RhIn type materials, especially with magnesium as main group element component. These results are promising. First investigations on Gd_4NiMg revealed hydrogen absorption up to $Gd_4NiMgH_{\sim 7}$ [26]. Systematic investigations are in progress.

The Gd_4RhIn type structure shows a large tolerance with respect to the valence electron concentration. In the indium based series these cubic compounds exist also with iridium as transition metal component [27]. The In_4 tetrahedra can be fully substituted by magnesium, as observed for the series of isotypic compounds RE_4CoMg (RE = Y, La, Pr, Nd, Sm, Gd–Tm) [15], RE_4RhMg (RE = Y, La–Nd, Sm, Gd–Tm, Lu) [16], and RE_4NiMg [26]. Also the cadmium compounds RE_4CoCd and RE_4RhCd (RE = Tb, Dy, Ho) with the rare motif of a Cd_4 tetrahedron have been synthesized and investigated with respect to their magnetic properties [24]. Recent phase analytical studies revealed that also the series RE_4RuMg, RE_4PdMg, RE_4PtMg, RE_4NiCd, and RE_4RuCd exist [25]. This offers the opportunity for tuning the magnetic properties as a function of the rare earth and transition metal component. Systematic studies on this exciting topic are in progress.

Experimental

Synthesis

Starting materials for the preparation of the RE_4RhIn indides were ingots of the rare earth metals (Johnson Matthey, Chempur or Kelpin), rhodium powder (*ca.* 200 mesh, Degussa-Hüls), and indium tear drops (Johnson Matthey), all with stated purities better than 99.9%. In a first step, the rare earth metal pieces were melted under 600 mbar argon to small buttons in an arc-melting furnace [10]. The argon was purified

Table 1. Lattice parameters (*Guinier* powder data) of the ternary indium compounds RE_4RhIn

Compound	a/pm	V/nm^3
Gd_4RhIn	1370.7(9)	2.5753
Tb_4RhIn	1360.3(6)	2.5171
Dy_4RhIn	1354.5(2)	2.4851
Ho_4RhIn	1349.2(3)	2.4560
Er_4RhIn	1342.5(5)	2.4196
Tm_4RhIn	1337.8(3)	2.3943
Lu_4RhIn	1329.7(3)	2.3511

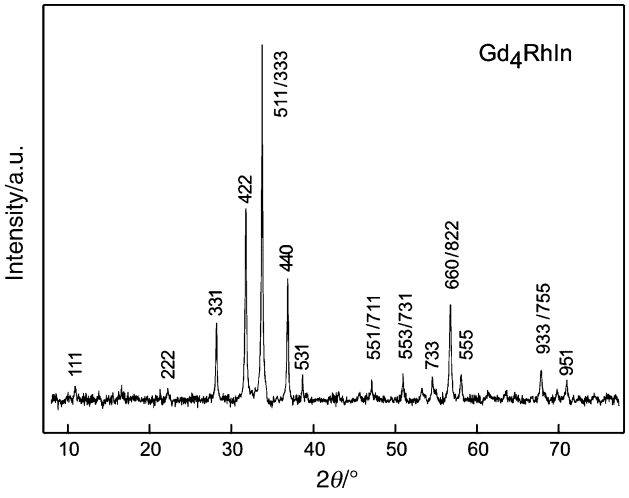

Fig. 4. *Guinier* powder pattern (CuK_{α_1} radiation) of Gd_4RhIn. The *hkl* indices of the strongest reflections are indicated

over titanium sponge (900 K), silica gel, and molecular sieves. The pre-melting procedure reduces shattering during the subsequent reactions with rhodium and indium. The rare earth metal buttons were then mixed with cold-pressed pellets (Ø 6 mm) of rhodium and pieces of the indium tear drops in the ideal 4:1:1 atomic ratio. The mixtures were reacted in the

Table 2. Crystal data and structure refinement for RE_4RhIn, space group $F\bar{4}3m$, $Z = 16$

Empirical formula	Gd_4RhIn	Tb_4RhIn	Dy_4RhIn
Molar mass	846.73 g/mol	853.41 g/mol	867.73 g/mol
Unit cell dimensions	Table 1	Table 1	Table 1
Calculated density	8.74 g/cm^3	9.01 g/cm^3	9.28 g/cm^3
Crystal size	$10 \times 30 \times 50$ μm^3	$15 \times 30 \times 200$ μm^3	$20 \times 20 \times 45$ μm^3
Detector distance	60 mm	–	100 mm
Exposure time	5 min	–	2 min
ω range; increment	0–180°; 1.0°	–	0–180°; 1.0°
Integr. param. A, B, EMS	13.5, 3.5, 0.012	–	13.5, 3.5, 0.014
Transm. ratio (max/min)	1.79	2.89	2.13
Absorption coefficient	46.5 mm^{-1}	50.4 mm^{-1}	53.6 mm^{-1}
$F(000)$	5600	5664	5728
θ range	2–30°	2–30°	2–29°
Range in hkl	±19, ±19, ±19	±19, ±19, ±19	±18, ±18, ±18
Total no. of reflections	6845	7390	8548
Independent reflections	428 ($R_{int} = 0.079$)	420 ($R_{int} = 0.059$)	380 ($R_{int} = 0.084$)
Reflections with $I > 2\sigma(I)$	374 ($R_\sigma = 0.039$)	420 ($R_\sigma = 0.017$)	304 ($R_\sigma = 0.064$)
Data/parameters	428/19	420/19	380/19
Goodness-of-fit on F^2	0.875	1.242	0.743
Final R indices [$I > 2\sigma(I)$]	$R1 = 0.026$	$R1 = 0.013$	$R1 = 0.023$
	$wR2 = 0.048$	$wR2 = 0.028$	$wR2 = 0.040$
R indices (all data)	$R1 = 0.032$	$R1 = 0.013$	$R1 = 0.034$
	$wR2 = 0.049$	$wR2 = 0.028$	$wR2 = 0.041$
Extinction coefficient	0.000168(9)	0.000168(4)	0.00029(1)
Flack parameter	0.01(4)	0.003(16)	−0.01(5)
Largest diff. peak and hole	3.41/−1.61 e/Å^3	3.10/−0.81 e/Å^3	3.87/−1.66 e/Å^3
Empirical formula	Ho_4RhIn	Er_4RhIn	Tm_4RhIn
Molar mass	877.45 g/mol	886.77 g/mol	893.45 g/mol
Unit cell dimensions	Table 1	Table 1	Table 1
Calculated density	9.49 g/cm^3	9.74 g/cm^3	9.91 g/cm^3
Crystal size	$20 \times 30 \times 200$ μm^3	$10 \times 20 \times 65$ μm^3	$10 \times 30 \times 90$ μm^3
Detector distance	–	60 mm	60 mm
Exposure time	–	5 min	5 min
ω range; increment	–	0–180°; 1.0°	0–180°; 1.0°
Integr. param. A, B, EMS	–	13.5, 3.5, 0.014	13.5, 3.5, 0.012
Transm. ratio (max/min)	3.09	2.54	2.84
Absorption coefficient	57.1 mm^{-1}	61.1 mm^{-1}	65.0 mm^{-1}
$F(000)$	5792	5856	5920
θ range	2–30°	3–30°	2–30°
Range in hkl	±18, ±18, ±18	±18, ±18, ±18	±18, ±18, ±18
Total no. of reflections	7154	6405	6205
Independent reflections	410 ($R_{int} = 0.071$)	403 ($R_{int} = 0.067$)	394 ($R_{int} = 0.059$)
Reflections with $I > 2\sigma(I)$	404 ($R_\sigma = 0.021$)	345 ($R_\sigma = 0.045$)	351 ($R_\sigma = 0.034$)
Data/parameters	410/19	403/19	394/19
Goodness-of-fit on F^2	1.183	0.802	0.904
Final R indices [$I > 2\sigma(I)$]	$R1 = 0.012$	$R1 = 0.020$	$R1 = 0.020$
	$wR2 = 0.029$	$wR2 = 0.036$	$wR2 = 0.037$
R indices (all data)	$R1 = 0.012$	$R1 = 0.028$	$R1 = 0.026$
	$wR2 = 0.029$	$wR2 = 0.037$	$wR2 = 0.038$
Extinction coefficient	0.00085(2)	0.000136(5)	0.000173(6)
Flack parameter	−0.008(14)	−0.01(3)	−0.03(3)
Largest diff. peak and hole	2.74/−0.84 e/Å^3	4.41/−1.66 e/Å^3	4.88/−1.58 e/Å^3

arc-furnace and remelted three times to ensure homogeneity. An additional synthesis was performed for the gadolinium compound with a starting composition 4.1:1:1 in order to getter a possible oxygen/nitrogen contamination (see above). The weight losses after the melting procedures were always smaller than 0.5%. The light gray polycrystalline samples are brittle and stable in air over months. Finely ground powders are dark gray and single crystals exhibit metallic luster.

Single crystals of the indides RE_4RhIn (RE = Gd–Tm) were grown *via* a special annealing sequence. First, the polycrystalline samples were powdered and cold-pressed into pellets. Next, the pellets were put in small tantalum containers that were sealed in evacuated silica tubes as an oxidation protection. The ampoules were first heated to 1300, 1305, 1305, 1310, 1340 and 1355 K for the compounds with Gd, Tb, Dy, Ho, Er and Tm as rare earth component, respectively, during 6 h and held at these temperatures for another 6 h. Subsequently, the temperature was lowered by 5 K/h–970 K in all cases, then at a rate of 15 K/h–670 K, and finally cooled to room temperature. Single crystals of irregular shape were selected. After cooling, the samples could easily be separated from the tantalum containers. No reaction of the samples with tantalum could be detected.

Scanning Electron Microscopy

The single crystals investigated on the diffractometers and the bulk samples have been analyzed by EDX measurements using a LEICA 420 I scanning electron microscope with the rare earth trifluorides, rhodium, and InAs as standards. Since the crystals were mounted by beeswax on glass fibres, they were first coated with a thin carbon film. The bulk samples were previously embedded in a metacrylate matrix and the surface was polished with different silica and diamond pastes. The surface remained unetched for the EDX measurements. No impurity elements were detected and the analyses were in agreement with the ideal 4:1:1 composition.

X-Ray Film Data and Structure Refinements

The RE_4RhIn samples were characterized through Guinier powder patterns using CuKα_1 radiation and α-quartz (a = 491.30, c = 540.46 pm) as an internal standard. The Guinier camera was equipped with an imaging plate system (Fujifilm BAS-1800). The cubic lattice parameters (Table 1) were deduced from least-squares fits of the powder data. To ensure correct indexing, the experimental patterns were compared to calculated ones [11], taking the atomic positions obtained from the structure refinements. As an example, a powder pattern of Gd_4RhIn is displayed in Fig. 4.

Small, irregularly shaped single crystals of Gd_4RhIn, Tb_4RhIn, Dy_4RhIn, Ho_4RhIn, Er_4RhIn, and Tm_4RhIn were selected from the annealed samples and examined by Laue photographs on a Buerger precession camera (equipped with an imaging plate system Fujifilm BAS-1800) in order to establish suitability for intensity data collection. Intensity data of Tb_4RhIn and Ho_4RhIn were recorded at room temperature by use of a four-circle diffractometer (CAD4) with graphite monochromatized MoK$_\alpha$ radiation (λ = 71.073 pm) and a scintillation counter with pulse-height discrimination. The scans were taken in the $\omega/2\theta$ mode and empirical absorption corrections were applied on the basis of psi-scan data followed by spherical absorption corrections. The data sets of the remaining crystals were collected in oscillation mode on a Stoe IPDS-II image plate diffractometer using monochromatized MoK$_\alpha$ radiation (71.073 pm). Numerical absorption corrections were applied to the data sets. All relevant crystallographic details for the data collections and evaluations are listed in Table 2.

Careful evaluation of the data sets revealed only the systematic extinctions for a face-centered lattice, leading to the possible space groups $Fm\bar{3}m$, $Fm\bar{3}$, $F\bar{4}3m$, and $F432$. The noncentrosymmetric group $F\bar{4}3m$ was found to be the correct one during structure refinement. The starting atomic parameters

Table 3. Atomic coordinates and isotropic displacement parameters (pm^2) of RE_4RhIn. U_{eq} is defined as one third of the trace of the orthogonalized U_{ij} tensor. Note the different absolute orientations

Atom	*Wyckoff* site	x	y	z	U_{eq}
Gd_4RhIn					
Gd1	24 *g*	0.56266(7)	1/4	1/4	73(2)
Gd2	24*f*	0.19002(7)	0	0	61(2)
Gd3	16*e*	0.34948(6)	x	x	58(3)
Rh	16*e*	0.14246(9)	x	x	73(4)
In	16*e*	0.58180(8)	x	x	69(3)
Tb_4RhIn					
Tb1	24 *g*	0.43672(3)	3/4	3/4	117(1)
Tb2	24*f*	0.81019(3)	0	0	102(1)
Tb3	16*e*	0.65009(2)	x	x	100(1)
Rh	16*e*	0.85739(4)	x	x	114(2)
In	16*e*	0.41786(3)	x	x	110(1)
Dy_4RhIn					
Dy1	24 *g*	0.56281(9)	1/4	1/4	68(3)
Dy2	24*f*	0.18915(9)	0	0	49(3)
Dy3	16*e*	0.35053(8)	x	x	56(3)
Rh	16*e*	0.14334(13)	x	x	66(5)
In	16*e*	0.58253(11)	x	x	64(4)
Ho_4RhIn					
Ho1	24 *g*	0.43736(3)	3/4	3/4	97(1)
Ho2	24*f*	0.81025(3)	0	0	81(1)
Ho3	16*e*	0.65007(2)	x	x	82(1)
Rh	16*e*	0.85740(4)	x	x	97(2)
In	16*e*	0.41740(3)	x	x	93(2)
Er_4RhIn					
Er1	24 *g*	0.43759(7)	3/4	3/4	58(2)
Er2	24*f*	0.81057(7)	0	0	40(2)
Er3	16*e*	0.64951(6)	x	x	44(2)
Rh	16*e*	0.8568(1)	x	x	53(4)
In	16*e*	0.41718(9)	x	x	47(3)
Tm_4RhIn					
Tm1	24 *g*	0.43822(6)	3/4	3/4	59(2)
Tm2	24*f*	0.81080(6)	0	0	39(2)
Tm3	16*e*	0.64902(5)	x	x	48(2)
Rh	16*e*	0.85642(9)	x	x	58(4)
In	16*e*	0.41700(8)	x	x	49(3)

Table 4. Interatomic distances (pm), calculated with the powder lattice parameters of Gd_4RhIn. Standard deviations are given in parentheses. All distances within the first coordination spheres are listed

Gd1:	2	In	327.1(3)	Gd3:	3	Rh	284.2(2)
	2	Rh	350.0(2)		3	In	345.2(3)
	2	Gd3	350.1(2)		3	Gd1	350.1(2)
	4	Gd2	362.7(2)		3	Gd2	364.6(3)
	4	Gd1	363.2(3)		3	Gd3	385.7(3)
Gd2:	2	Rh	283.7(2)	Rh:	3	Gd2	283.7(2)
	2	In	350.7(3)		3	Gd3	284.2(2)
	4	Gd1	362.7(2)		3	Gd1	350.0(2)
	2	Gd3	364.6(3)	In:	3	In	317.1(4)
	4	Gd2	368.4(3)		3	Gd1	327.1(3)
					3	Gd3	345.2(3)
					3	Gd2	350.7(3)

for Gd_4RhIn were deduced from an automatic interpretation of direct methods with SHELXL-97 [12] and the structure was refined using SHELXL-97 (full-matrix least-squares on $F_0{}^2$) [13] with anisotropic atomic displacement parameters for all sites. The structural parameters were then standardized with the TYPIX routine [14] and all remaining data sets were refined with the same setting. As a check for the correct site assignments (rhodium and indium differ by only four electrons) and possible mixed occupancies [15, 16] the occupancy parameters were refined in separate series of least-squares cycles. All sites were fully occupied within two standard uncertainties, and in the final cycles the ideal occupancies were assumed again. The refinements went smoothly to the residuals listed in Table 2. Refinement of the correct absolute structures was ensured through refinement of the Flack parameters [17, 18]. Final difference Fourier syntheses revealed no significant residual peaks (Table 2). The positional parameters and interatomic distances (exemplary for Gd_4RhIn) are listed in Tables 3 and 4. Further details on the structure refinements are available*.

Acknowledgements

We thank *H.-J. Göcke* for the work at the scanning electron microscope. This work was financially supported by the Deutsche Forschungsgemeinschaft.

References

[1] Kalychak YaM, Zaremba VI, Pöttgen R, Lukachuk M, Hoffmann R-D (2005) Rare Earth-Transition Metal-Indides. In: Gschneider KA Jr, Pecharsky VK, Bünzli J-C (eds) Handbook on the Physics and Chemistry of Rare Earths. Vol. 34, chapter 218, pp 1–133, Elsevier, Amsterdam
[2] Gladyshevsky RE, Grin YuN, Yarmolyuk YaP (1983) Dopov Akad Nauk Ukr RSR Ser A **45**: 67
[3] Zaremba VI, Kalychak YaM, Zavalii PYu (1992) Sov Phys Crystallogr **37**: 178
[4] Canepa F, Napoletano M, Fornasini ML, Merlo F (2002) J Alloys Compd **345**: 42
[5] Zaremba VI, Kalychak YaM, Dzevenko MV, Rodewald UCh, Heying B, Pöttgen R (2006) Z Naturforsch **61b**: 23
[6] Kalychak YaM, Zaremba VI, Stępień-Damm J, Galadzhun YaV, Akselrud LG (1998) Kristallografia **43**: 17 (in Russian)
[7] Galadzhun YaV, Zaremba VI, Kalychak YaM, Davydov VM, Pikul AP, Stępień-Damm J, Kaczorowski D (2004) J Solid State Chem **177**: 17
[8] Aronsson B (1958) Acta Chem Scand **12**: 31
[9] Bertaut F, Blum P (1953) CR Acad Sci Paris **236**: 1055
[10] Pöttgen R, Gulden Th, Simon A (1999) GIT Labor Fachzeitschrift **43**: 133
[11] Yvon K, Jeitschko W, Parthé E (1977) J Appl Crystallogr **10**: 73
[12] Sheldrick GM (1997) SHELXS-97, Program for the Solution of Crystal Structures, University of Göttingen
[13] Sheldrick GM (1997) SHELXL-97, Program for Crystal Structure Refinement, University of Göttingen
[14] Parthé E, Gelato L, Chabot B, Penzo M, Cenzual K, Gladyshevskii R (1993) TYPIX-Standardized Data and Crystal Chemical Characterization of Inorganic Structure Types. Gmelin Handbook of Inorganic and Organometallic Chemistry, 8th edn. Springer, Berlin
[15] Tuncel S, Hoffmann R-D, Chevalier B, Matar SF, Pöttgen R (2007) Z Anorg Allg Chem **633**: 151
[16] Tuncel S, Rodewald UCh, Chevalier B, Pöttgen R (2007) Z Naturforsch **626**: 642
[17] Flack HD, Bernadinelli G (1999) Acta Crystallogr **55A**: 908
[18] Flack HD, Bernadinelli G (2000) J Appl Crystallogr **33**: 1143
[19] Emsley J (1999) The Elements. Oxford University Press, Oxford
[20] Donohue J (1974) The Structures of the Elements. Wiley, New York
[21] Lokken DA, Corbett JD (1973) Inorg Chem **12**: 556
[22] Simon A, Holzer N, Mattausch Hj (1979) Z Anorg Allg Chem **456**: 207
[23] Simon A (1994) Discrete and Condensed Transition Metal Clusters in Solids. In: Schmid G (ed) Clusters and Colloids. From Theory to Applications, VCH, Weinheim
[24] Doğan A, Rayaprol S, Pöttgen R (2007) J Phys Condens Matter **19**: 076213
[25] Schappacher F, Tuncel S, Doğan A, Chevalier B, Pöttgen R (unpublished results)
[26] Chevalier B, Bobet J-L, Tuncel S, Pöttgen R (unpublished results)
[27] Zaremba R, Rodewald UCh, Pöttgen R (2006) Z Anorg Allg Chem **632**: 2106

* Details may be obtained from: Fachinformationszentrum Karlsruhe, D-76344 Eggenstein-Leopoldshafen (Germany), by quoting the Registry Nos. CSD-417516 (Gd_4RhIn), CSD-417518 (Tb_4RhIn), CSD-417514 (Dy_4RhIn), CSD-417517 (Ho_4RhIn), CSD-417515 (Er_4RhIn), and CSD-417519 (Tm_4RhIn)